

Supporting Information

Bacterial microenvironment-responsive dual-channel smart imaging guided on-demand self-regulated photodynamic/chemodynamic synergistic sterilization and wound healing

Xu Zhao,^{*123} Xiang Wei,³ Li-Jian Chen,¹²³ and Xiu-Ping Yan¹²³⁴

¹State Key Laboratory of Food Science and Technology, Jiangnan University, Wuxi 214122, China

² International Joint Laboratory on Food Safety, Jiangnan University, Wuxi 214122, China

³ Institute of Analytical Food Safety, School of Food Science and Technology, Jiangnan University, Wuxi 214122, China

⁴ Key Laboratory of Synthetic and Biological Colloids, Ministry of Education, School of Chemical and Material Engineering, Jiangnan University, Wuxi, 214122, China

*Corresponding authors. E-mail: zhaoxu2017@jiangnan.edu.cn

Supplementary Methods

Chemicals and materials. Germanium oxide (GeO_2), manganese nitrate ($\text{Mn}(\text{NO}_3)_2$), zinc nitrate ($\text{Zn}(\text{NO}_3)_2$), *N, N*-dimethylformamide (DMF), cetyltrimethyl ammonium bromide (CTAB) and ethanol were bought from Sinopharm Chemical Reagent Co. Ltd. (Shanghai, China). Piperazine functionalized polyethylene glycol (Mal-PEG-piperazine) was obtained from Xi'an Ruixi Biological Technology Co. Ltd. (Xi'an, China). Methylene blue (MB) was purchased from Macklin Co. Ltd. (Shanghai, China). 1,3-diphenylisobenzofuran (DPBF) was bought from Energy Chemical (Shanghai, China). 2',7'-dichlorodihydrofluorescein diacetate (DCFH-DA) and singlet oxygen sensor green (SOSG) were purchased from Aladdin Reagent Co. Ltd (Shanghai, China). Singlet oxygen fluorescence probe was provided by Maokang Biotechnology Co. Ltd (Shanghai, China). 3-(4,5-Dimethyl-thiazol-2-yl)-2,5-diphenyltetrazolium bromide (MTT), 4',6-diamidino-2-phenylindole (DAPI), Calcein acetoxymethyl ester and propidium iodide (Calcein-AM/PI) live and dead bacteria detection kit and mercaptopropyl trimethoxysilane (MPTES) were supplied from Sigma-Aldrich Co. LLC (Shanghai, China). Culture medium and consumables for cell culture were supplied by Dingguo Biotechnology Co. (Beijing, China). *Escherichia coli* (*E. coli*, ATCC 25922), *Staphylococcus aureus* (*S. aureus*, ATCC 25923) were thawed from the frozen bacteria in our laboratory. Other reagents were of at least of analytical grade and used without further purification.

Instrumentation and characterization. Fourier transform infrared (FT-IR) spectra were carried out on a Nicolet IS50 spectrometer (Thermo, America) by using KBr pellet. X-ray diffraction spectra were obtained from a D2 PHASER diffractometer (Bruker AXS, Germany). Phosphorescence and fluorescence spectra were performed on an F-7000 spectrofluorometer (Hitachi, Japan). Absorption spectra were recorded on a UV 3600 PLUS UV-Vis-

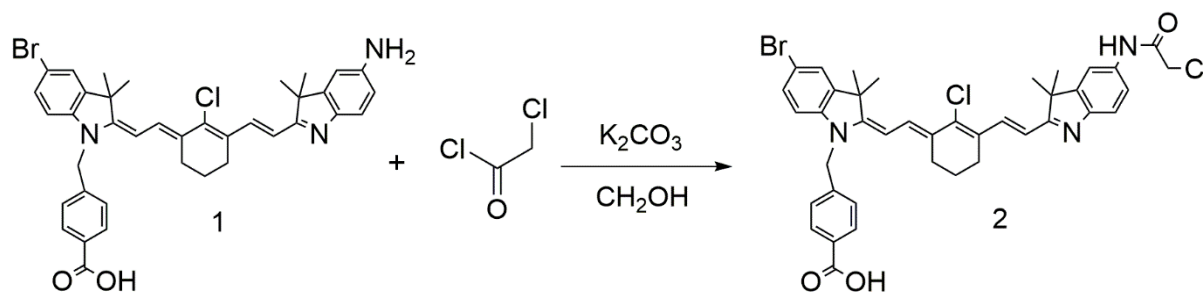
NIR spectrometer (Shimadzu, Japan). Mass spectrometry was acquired on the QTRAP 4500 LC-MS/MS (Thermo, America). Transmission electron microscopy images (TEM) were obtained at 200 kV with a JEM-2100 TEM (JEOL, Japan). Zeta potential and hydrodynamic size distribution were measured on a ZEN3700 Nano laser particle size analyzer (Marvin, England). Electron spin resonance (ESR) images were determined by EMXplus-10/12 spectrometer (Bruker, Germany). Bacterial imaging was acquired on a FV3000 confocal laser scanning microscope (Olympus, Japan). Scanning electron microscopy images (SEM) were obtained with a SU8100 SEM (Hitachi, Japan). Absorbance for the MTT assay was recorded on a Synergy H1 microplate reader (BioTek, USA) at a wavelength of 570 nm. *In vivo* phosphorescence and fluorescence imaging of mice were carried out on an IVIS Lumina III imaging system (PerkinElmer, America). The concentration of C-reactive protein (CRP) was measured by the CRP ELISA kit.

Preparation of PLNP:

Zn₂GeO₄:Mn nanorods were prepared according to the reference method with a slight modification.^[1] Firstly, 0.5 mol L⁻¹ of Zn(NO₃)₂, 0.4 mol L⁻¹ of Na₂GeO₃ and 0.043 mol L⁻¹ of Mn(NO₃)₂ solutions were prepared respectively. Among them, Na₂GeO₃ solution was prepared by dissolving germanium oxide in sodium hydroxide solution (5 mmol L⁻¹), other solutions were prepared by Wahaha mineral water. Zn(NO₃)₂ (16 mmol, 32 mL) and Mn(NO₃)₂ (0.04 mmol, 928 μL) were placed in a round-bottom flask and then the mixture was diluted to 88 mL with water. 2.4 mL of concentrated HNO₃, 20 mL of Na₂GeO₃ (8 mmol) and 128 mg of CTAB were slowly added in sequence under vigorous agitation. Then the pH of the solution was rapidly adjusted to 9.0 with ammonium hydroxide (25%, wt). After stirring at room temperature for 1 h, the mixture was transferred to the Teflon-lined stainless steel autoclave and reacted at 220°C for 6 h. After cooling to room temperature,

the resultant was collected by centrifugation at 10000 rpm for 10 min and washed alternately with ethanol and water for 6 times. Finally, the prepared PLNP was lyophilized and stored for further use.

Synthesis of PS:



Compound 1 was prepared according to the previous reported method.^[2] 50 mg of compound 1 was dissolved in 50 mL ethanol, followed by the addition of chloroacetyl chloride and potassium carbonate to maintain an alkaline environment and reacted at room temperature for 3 h. After the reaction, the excess solvent was removed by rotary evaporation first, and then the mixture was poured into water and extracted with dichloromethane. Finally, the title compound was obtained by combination and concentration of the organic phases without further purification.

Preparation of PLNP-PS:

The prepared PLNP was dispersed in NaOH solution (5 mmol L⁻¹) by ultrasound for 10 min first, and then vigorously stirred for 24 h. PLNP-OH was obtained by washing the centrifugally collected products alternately with ethanol and water for three times. Then, the obtained PLNP-OH was ultrasonically dispersed in DMF at a concentration of 2 mg mL⁻¹. After 10 min of ultrasound, MPTES were dropped under stirring at the ratio of 8 μL MPTES per mL of reaction solution, and then the reaction mixture was conducted at 80°C for 24 h. The reaction solution was centrifuged and washed with DMF and ethanol alternately for 3 and then dried at room temperature to offer PLNP-SH.

The obtained PLNP-SH was ultrasonically dispersed in PBS at a concentration of 2 mg mL⁻¹, and Mal-PEG-piperazine was added and stirred overnight. PLNP-PEG was obtained by centrifugation, and washing with water and ethanol for three times. The lyophilized PLNP-PEG was ultrasonically dispersed in DMF and PS was added for reaction at 70 °C for 3 h under N₂ atmosphere. The precipitate obtained by centrifugation was washed alternately with water and ethanol for three times, wrapped in tin foil and lyophilized to obtain the dark purple final product PLNP-PS.

Acid degradation properties of PLNP-PS:

In order to study the acid-responsive degradation characteristic of PLNP-PS, the phosphorescence/fluorescence intensity was detected by fluorescence spectrophotometer and IVIS Lumina III imaging system, and the morphology was detected by TEM. The solution of PLNP and PLNP-PS (0.4 mg mL⁻¹) were prepared with PBS buffer solution (10 mmol L⁻¹, pH 6.0, pH 6.5 and pH 7.4, respectively). And then 500 μL of solution was taken to measure its phosphorescence/fluorescence at different time points (0 h, 0.5 h, 1 h, 2 h, 3 h, 4 h, 5 h, 6 h, 8 h, and 24 h, respectively). The detection conditions were as follows: the excitation and emission slits were 10 nm, and the voltage was 500V.

To evaluate the acid-responsive phosphorescence/fluorescence images of PLNP-PS by using IVIS Lumina III imaging system, each solution (200 μL, n=3) was added into a black 96-well plate. The phosphorescence/fluorescence images of each was monitored well at different times (0 h, 0.5 h, 1 h, 2 h, 3 h, 4 h, 5 h, 6 h, 8 h and 24 h, respectively) before 10 min of pre-excited with UV lamp (6W).

Electron microscopic samples were prepared from the above solution at different time points (0 h, 2 h, 4 h, 6 h and 24 h, respectively) and photographed.

Charge conversion of PLNP-PS:

PLNP and PLNP-PS were dispersed into PBS buffer solution (0.5 mmol L^{-1}) at pH 6.0, pH 6.5 and pH 7.4, respectively to a final concentration of 0.2 mg mL^{-1} . The zeta potential of each solution was measured by nano laser particle size analyzer after ultrasonic dispersion.

Chemodynamic properties of PLNP-PS:

To investigate the chemodynamic performance, the ion release of PLNP and PLNP-PS under simulated bacterial acidic microenvironment or normal physiological pH was detected by ICP-MS first. PLNP and PLNP-PS were dispersed with PBS (pH 6.0, pH 6.5 and pH 7.4, 10 mmol L^{-1} , respectively) to a concentration of 0.4 mg mL^{-1} , respectively. The ion concentration of the above solutions was detected by ICP-MS at different time points (0 h, 0.5 h, 1 h, 2 h, 3 h, 4 h, 5 h, 6 h, 8 h and 24 h, respectively).

MB, a sensitive probe of reactive oxygen species (ROS), was then chosen as an indicator to evaluate the chemodynamic properties. The PLNP-PS solution (10 mg mL^{-1}) were dispersed with PBS (pH 7.4/6.0) and stored at room temperature for 4 hours. The supernatant was centrifuged for further use. Transfer $200 \text{ }\mu\text{L}$ of MB ($100 \text{ }\mu\text{g mL}^{-1}$), H_2O_2 (100 mmol L^{-1}) and NaHCO_3 (250 mmol L^{-1}) to a 2-mL centrifuge tube, and then $0 \text{ }\mu\text{L}$, $20 \text{ }\mu\text{L}$, $80 \text{ }\mu\text{L}$, $160 \text{ }\mu\text{L}$ or $200 \text{ }\mu\text{L}$ (pH 7.4/6.0) of PLNP-PS supernatant was added, respectively. After that the mixture was diluted with water to 2-mL. The absorbance changes at 664 nm were detected after shaking at 37°C for 4 h in the dark. In addition, the absorbance of different solutions at 663 nm was measured: 1) MB+ NaHCO_3 ; 2) MB+ NaHCO_3 + H_2O_2 ; 3) MB+ NaHCO_3 + H_2O_2 +PLNP, pH 7.4; 4) MB+ NaHCO_3 + H_2O_2 +PLNP-PS, pH 7.4; 5) MB+ NaHCO_3 + H_2O_2 +PLNP, pH 6.0; 6) MB+ NaHCO_3 + H_2O_2 +PLNP-PS, pH 6.0. What's more, transferring $200 \text{ }\mu\text{L}$ of MB, H_2O_2 and NaHCO_3 and $80 \text{ }\mu\text{L}$ of PLNP-PS supernatant to a 2-mL centrifuge tube, and then the mixture was diluted with water to 2-mL and mixed evenly. The absorbance changes at 664 nm were

detected after shaking at 37°C for different time (0 min, 20 min, 40 min, 60 min, 90 min, 120 min, 180 min, and 240 min, respectively) in the dark.

Photodynamic properties of PLNP-PS:

To investigate the photodynamic performance of PLNP-PS, DPBF, a universal probe of singlet oxygen ($^1\text{O}_2$), was used as an indicator. Briefly, 100 μL of PLNP-PS with different concentrations (1 mg mL^{-1} , 4 mg mL^{-1} and 10 mg mL^{-1} , respectively) was mixed with DPBF solution ($6 \times 10^{-5} \text{ mol L}^{-1}$ in acetonitrile, 900 μL), and the resulting solution was adjusted to pH 6.0 by HCl (1 mol L^{-1}). The above solutions were then irradiated with 808 nm laser (0.6 W cm^{-2}) for different times (0 s, 10 s, 20 s, 30 s, 40 s, 50 s, 60 s, 90 s, 120 s, 180 s, 300 s and 600 s, respectively). Meanwhile, the absorption spectra of each solution were measured by UV-Vis-NIR spectroscopy after irradiation. The blank and control groups were carried out with the following parallel groups and irradiated under the same conditions: DPBF ($6 \times 10^{-5} \text{ mol L}^{-1}$, pH 6.0 or pH 7.4), 100 μL of PLNP (4 mg mL^{-1} , pH 6.0 or pH 7.4) with 900 μL of DPBF ($6 \times 10^{-5} \text{ mol L}^{-1}$) or PLNP-PS (4 mg mL^{-1} , pH 7.4) with 900 μL of DPBF ($6 \times 10^{-5} \text{ mol L}^{-1}$).

***In Vitro* Antibacterial Effect:**

To evaluate the in vitro antibacterial effect of effect, *E. coli* and *S. aureus* were selected as model organism, and further experiments were carried out after culture to exponential growth stage. The concentration of bacteria was determined based on the flat colony counting method.

The optimal co-incubation time was detected by using confocal microscopy (CLSM). Briefly, 5 mL of bacterial suspension was centrifuged at 4000 rpm for 10 min, and re-suspended in 1-mL LB (pH 7.4/6.0) containing 0.4 mg mL^{-1} of PLNP or PLNP-PS, respectively. After different incubation times (1 h, 2 h, 3 h, 4 h, 5 h, 7 h, 9 h and 12 h, respectively) at 37°C, 100 μL of bacterial suspension was taken from each group and centrifuged (5000 rpm, 3 min),

followed by re-suspended with PBS (50 μL). Finally, 10 μL of bacterial solution was dropped onto a glass slide and covered with a coverslip for CLSM images.

Two model strains (both 10^8 CFU mL^{-1} , 900 μL) in LB were mixed with 100- μL PLNP-PS solution with different concentration (1 mg mL^{-1} , 4 mg mL^{-1} , 8 mg mL^{-1} and 10 mg mL^{-1} , respectively) and incubated for 4 h. After incubation, 100 μL of bacterial suspension was taken and diluted 10^5 times with PBS gradiently. Then 100 μL of diluted bacterial suspension were added to LB agar plate and incubated in an aerophilic environment at 37°C for 24 h. Bacteria treated with the same process with 100 μL PBS were used as blank control. The dark toxicity of PLNP (0.1 mg mL^{-1} , 0.4 mg mL^{-1} , 0.8 mg mL^{-1} and 1.0 mg mL^{-1} , respectively) on the two strains was investigated using the same method.

To investigate the chemodynamic/photodynamic antibacterial effect, *E. coli* or *S. aureus* suspension treated with PLNP-PS or not were divided into the following groups: Experimental group: Bacteria treated with PLNP-PS and H_2O_2 in LB medium (pH 6.0) and exposed to an 808 nm laser (0.6 W cm^{-2} , 10 min). A series of control groups as follow: Bacteria in LB (pH 6.0); Bacteria in LB (pH 6.0) with H_2O_2 ; Bacteria in LB (pH 6.0) with 808 nm laser irradiation; Bacteria in LB (pH 6.0) with H_2O_2 and 808 nm laser irradiation and Bacteria treated with PLNP-PS in LB (pH 7.4) with H_2O_2 and 808 nm laser irradiation; Bacteria treated with PLNP solution (0.4 mg mL^{-1}) also grouped as described above. Then the bacterial culture method was similar to the dark toxicity test.

To further verify the photodynamic and chemodynamic effects of PLNP-PS, the bacteria in the experimental group and control group were stained with Calcein-AM /PI live and dead bacteria staining kit. The bacteria were incubated with 50 μL Calcein-AM ($2 \mu\text{mol L}^{-1}$) and 50 μL PI ($3 \mu\text{mol L}^{-1}$) for 15 min. After centrifugation, it was re-suspended in PBS. CLSM imaging was then performed on a slide with 10 μL of re-suspended droplets.

To further verify the antibacterial mechanism of PLNP-PS, DCFH-DA and SOSG were employed as ROS and $^1\text{O}_2$ indicator, respectively. For this purpose, DCFH (20 μL) solution and PLNP/PLNP-PS or LB (100 μL) were added to 880 μL bacterial suspension (10^8 CFU mL^{-1}) in the presence or absence of H_2O_2 . In addition, the above experiment was also carried out after SOSG (10 μL) solution replaced DCFH. After incubation at 37°C for 4 h, the bacteria solution was irradiated with 808 nm laser (0.6 W cm^{-2}) for 10 min or not. Then the bacterial suspension was centrifuged (10000 rpm, 3 min) and re-suspended with PBS for CLSM images. The treatment methods of other control groups were the same as above.

Cytotoxicity Evaluation:

To evaluate the cytotoxicity of PLNP-PS, standard MTT assay was carried out using mouse embryonic fibroblast (3T3) as the representative mammalian host cell line. Briefly, 3T3 cell (100 μL , 10^5 cells mL^{-1} in DMEM) was planted in 96-well plate and incubated overnight. Then the culture medium was replaced with 100 μL of fresh medium contained various concentration of PLNP-PS (0.1 mg mL^{-1} , 0.4 mg mL^{-1} , 0.8 mg mL^{-1} or 1.0 mg mL^{-1} , respectively) for another 24 h incubation. The cells incubated with fresh medium only were served as blank control. Afterwards, the original medium was replaced with MTT solution (0.5 mg mL^{-1} , 100 μL). After incubation for 4 h, the supernatant was discarded. Meanwhile, 100 μL of DMSO was added into each well and the absorbance was measured by a microplate reader at a wavelength of 570 nm. In addition, the cytotoxicity of PLNP was studied by the same method.

***In Vivo* phosphorescence/Fluorescence Imaging of *S. aureus*-Infected Mice:**

Female BALB/C (5-6 weeks) was purchased Jiangsu Changzhou Kaswin Experimental Animal Co. Ltd. All experiments were performed in strict accordance with Chinese National Standard Laboratory Animal-Guideline for ethical review of animal welfare (GB/T 35892-2018) and

were approved by the Institutional Animal Care and Use Committee of Jiangnan University (Wuxi, China).

To evaluate the phosphorescence degradation indicator function of PLNP-PS *in vivo*, mouse wound model infected with *S. aureus* was established. The specific procedures were as follows: A wound with a diameter of about 7 mm was cut on the back of mice, and *S. aureus* (10^7 CFU mL⁻¹, 10 μ L) suspended in PBS was dropped and incubated for 12 h. Mice were randomly divided into 4 groups (n=6), which were left untreated or coated with 100 μ L blank gel, PLNP gel or PLNP-PS gel, respectively. Three mice in each group were randomly selected and irradiated with 808 nm laser for 10 min after coating with gel for 4 h. The mice were anesthetized at different time points (0 h, 0.5 h, 1 h, 2 h, 3 h, 4 h, 6 h, 8 h and 24 h, respectively) and the changes of phosphorescence at the wound of each group were monitored by IVIS imaging system.

***In Vivo* Chemodynamic/Photodynamic Synergetic Sterilization Effect:**

To study the effect of *in vivo* chemodynamic/photodynamic therapy, mice with infected wounds were randomly divided into 8 groups (n=3): Experimental group: Mice wounds coating with PLNP-PS gel and with 808 nm laser irradiation. Control groups: Mice without treatment; mice without gel and with 808 nm laser irradiation; coating with blank gel; coating with blank gel and irradiated with 808 nm laser; coating with PLNP gel; coating with PLNP gel and irradiated with 808 nm laser; coating with PLNP-PS gel. 808 nm laser irradiation (0.6 W cm⁻², 10 min) was applied to the wounds after applying the gel for 4 h. Mice of each group were photographed and weighed daily, until the wounds of mice in the experimental group were completely healed. The wound size of mice was measured by Image J software.

After the whole therapeutic process, the mice were euthanized. The main organs (heart, liver, spleen, lung and kidney) were dissected and the skin of the wound was cut and fixed in

4% paraformaldehyde solution for H&E staining to evaluate the potential side effects of the prepared PLNP-PS.

In addition, to further confirm the therapeutic efficiency of PLNP-PS for bacterial infection, the C-reactive protein (CRP) in the serum of each group after 8 d treatment was measured through CRP ELISA kit.

Supplementary References.

1. J. Wang, Q. Ma, W. Zheng, H. Liu, C. Yin, F. Wang, X. Chen, Q. Yuan, and W. Tan. *ACS Nano* 2017, **11**, 8185-8191.
2. X. Zhao, K. C. Zhao, L. J. Chen, Y. S. Liu, J. L. Liu, and X. P. Yan. *Chem. Sci.* 2020, **12**, 442-452.

Supplementary Figures

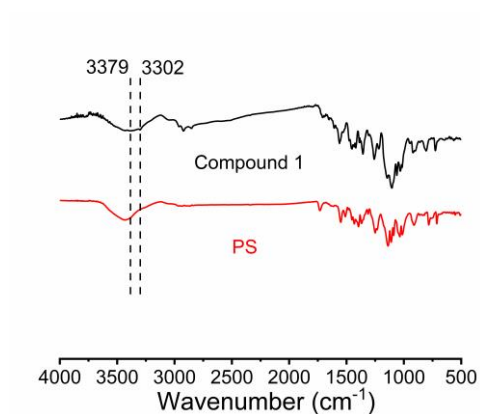


Figure S1. FT-IR spectrum of compound 1 and PS.

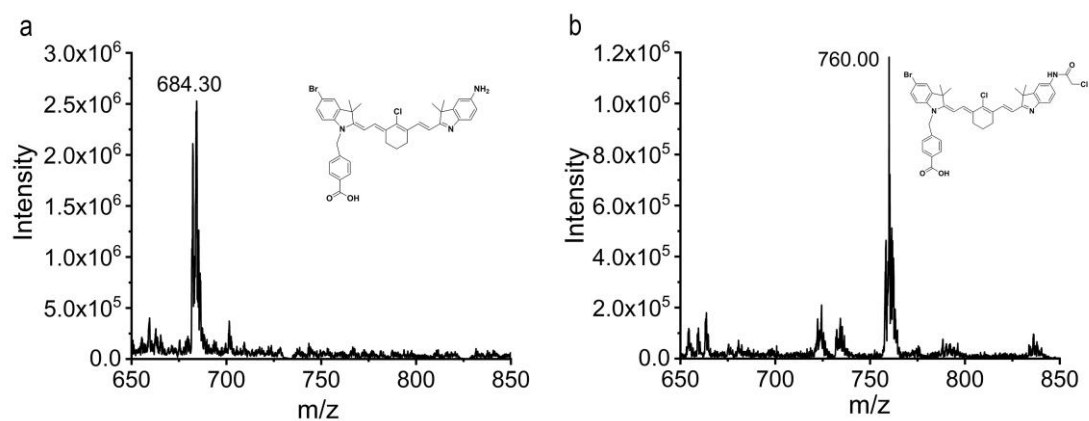


Figure S2. Mass spectra of (a) compound 1 and (b) PS.

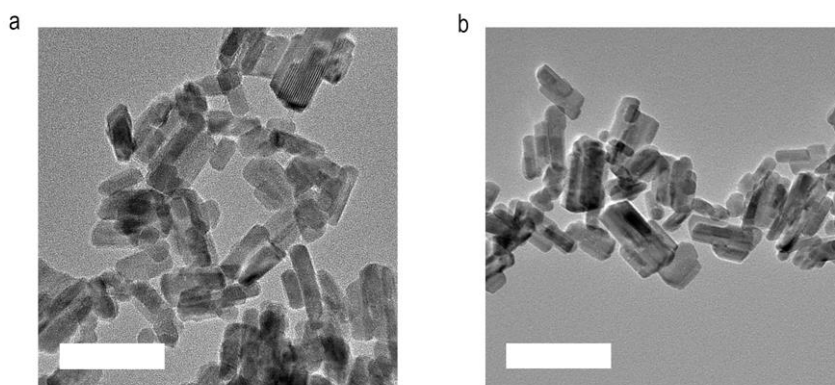


Figure S3. Transmission electron microscopy image (TEM) of (a) PLNP and (b) PLNP-PS (Scale bar, 100 nm).

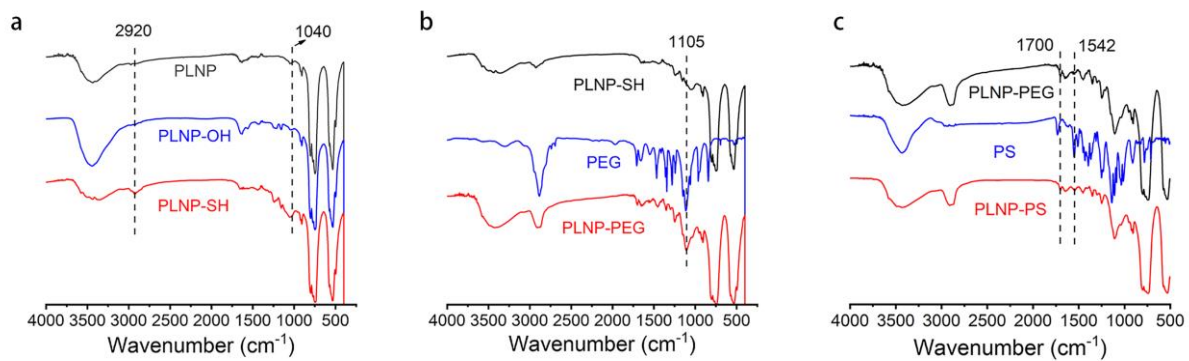


Figure S4. (a) FT-IR spectra of PLNP, PLNP-OH and PLNP-SH. (b) FT-IR spectra of PLNP-SH, PEG and PLNP-PEG. (c) FT-IR spectra of PLNP-PEG, PS and PLNP-PS.

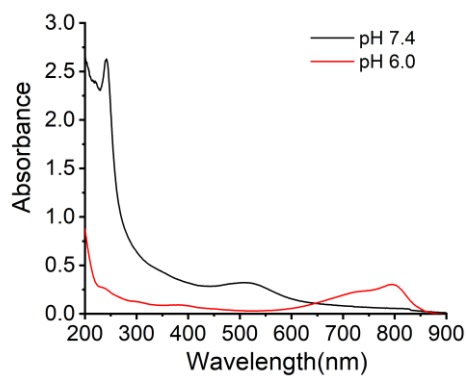


Figure S5. UV-vis-NIR absorption spectra of PLNP-PS (0.4 mg mL^{-1}) at pH 7.4 and 6.0.

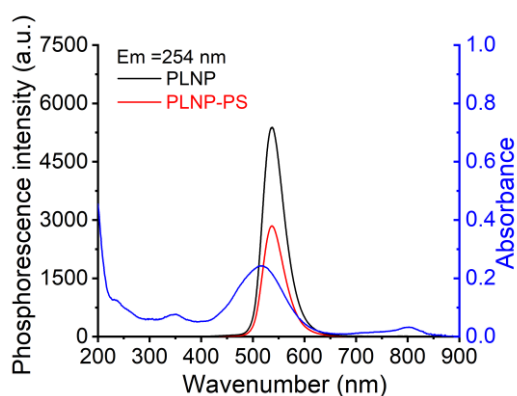


Figure S6. Emission spectra of PLNP, PLNP-PS and UV-vis-NIR absorption spectrum of the corresponding concentration PS grafted on PLNP-PS at pH 7.4.

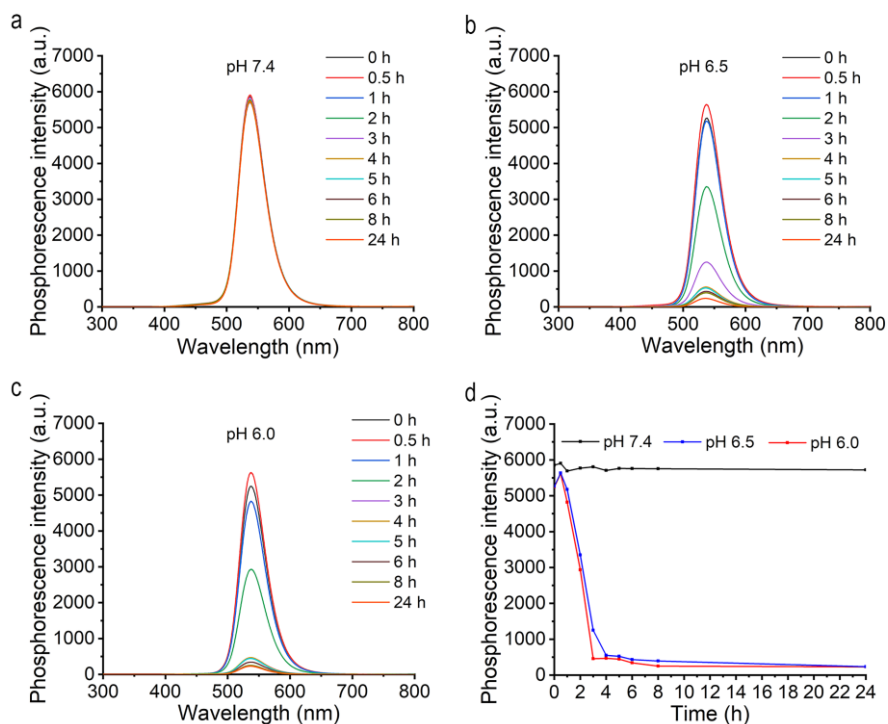


Figure S7. Time-dependent phosphorescence change curves of PLNP at different pH.

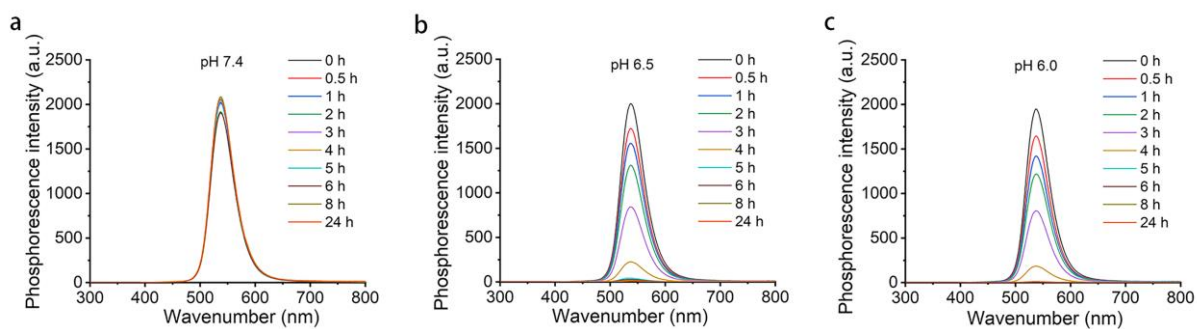


Figure S8. Time-dependent phosphorescence change curves of PLNP-PS at different pH.

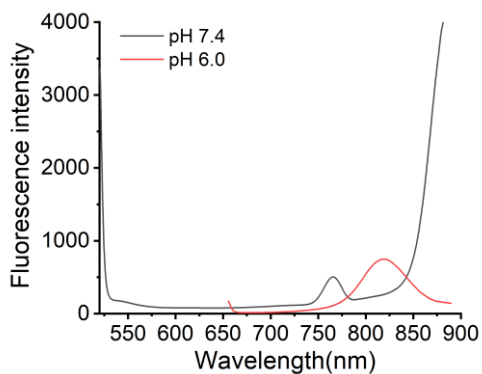


Figure S9. Fluorescence spectra of PS ($1.47 \times 10^{-6} \text{ mol L}^{-1}$) at pH 7.4 and 6.0.

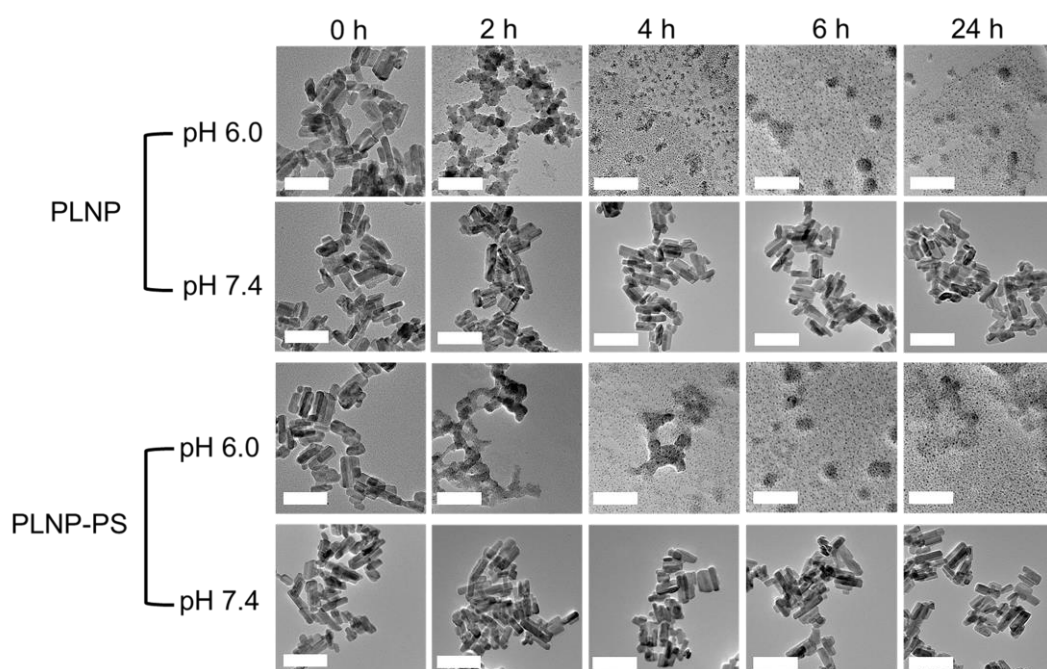


Figure S10. TEM images of PLNP and PLNP-PS at different pH in different times (Scale bar, 100 nm).

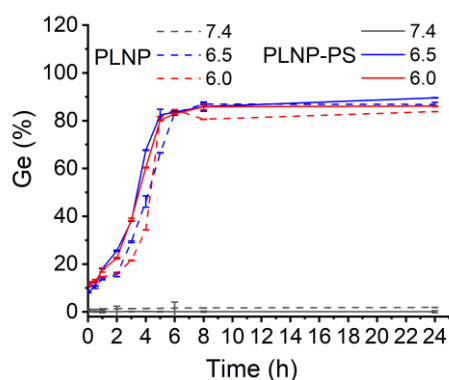


Figure S11. Release of Ge ion of PLNP and PLNP-PS at different pH with time.

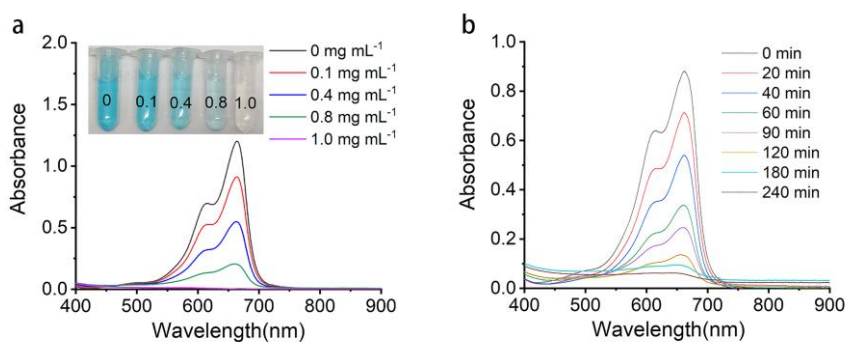


Figure S12. Time-dependent absorption spectra changes of PLNP-PS with (a) different concentrations and (b) times.

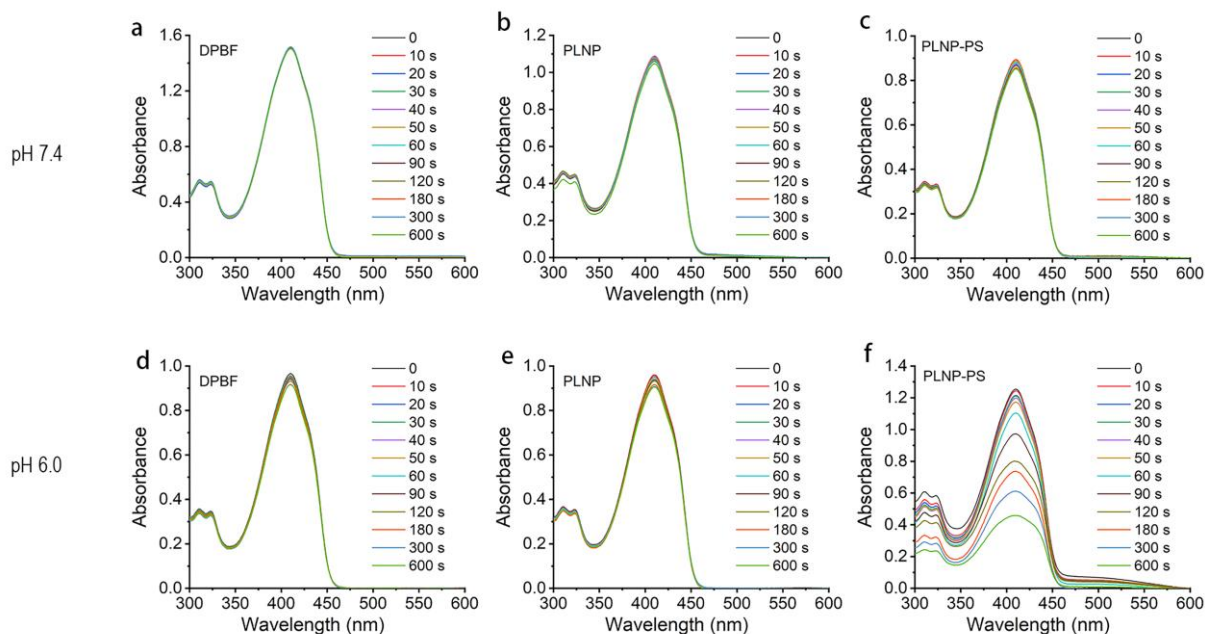


Figure S13. Time-dependent absorption spectra changes of DPBF with or without PLNP or PLNP-PS at pH 7.4 or 6.0 under 808 nm laser irradiation (0.6 W cm^{-2}).

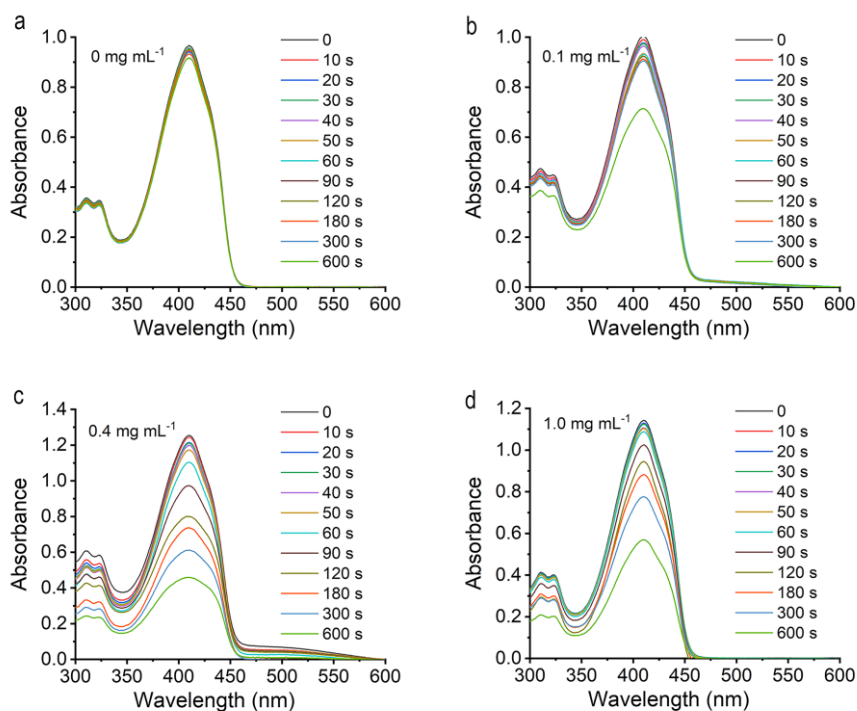


Figure S14. Time-dependent absorption spectra changes of DPBF at 410 nm with or without different concentrations of PLNP-PS at pH 6.0 under 808 nm laser irradiation (0.6 W cm^{-2}).

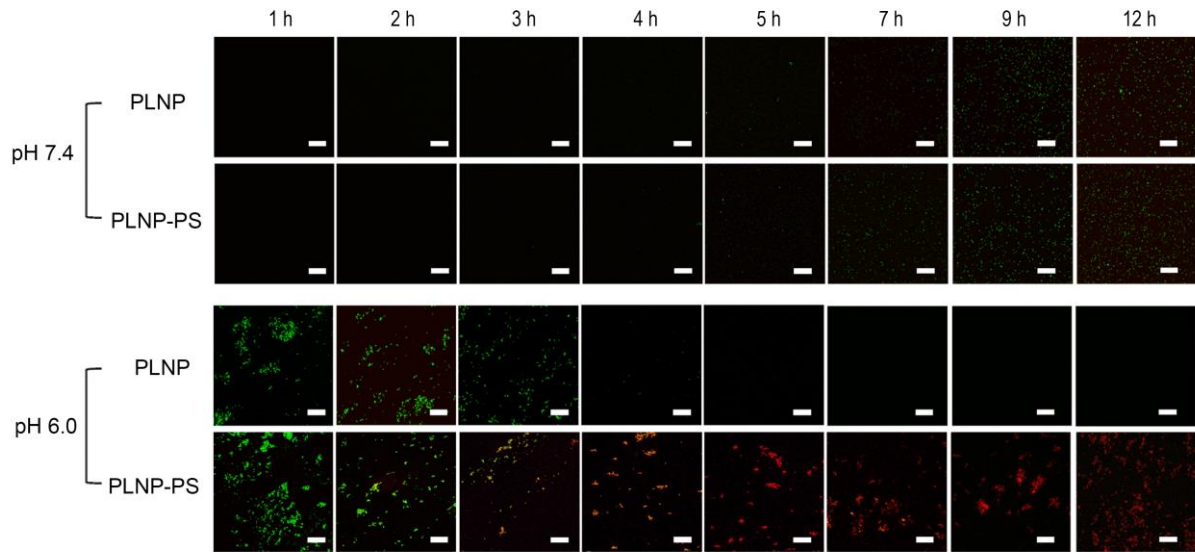


Figure S15. CLSM images of *S. aureus* treated with PLNP or PLNP-PS at pH 7.4 or 6.0.

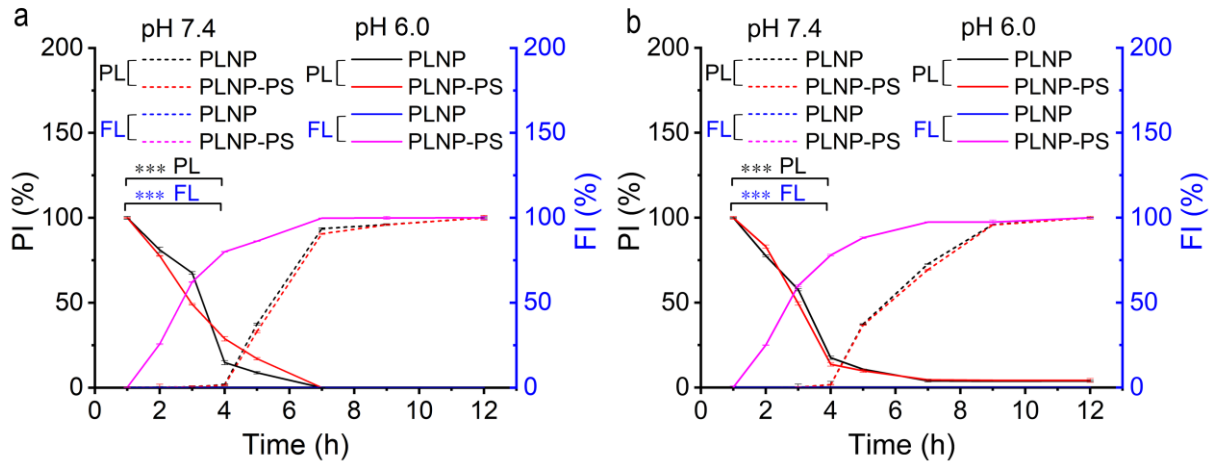


Figure S16. Time dependent phosphorescence (green) /fluorescence (red) intensity changes of PLNP and PLNP-PS in (a) *E. coli* and (b) *S. aureus* was measured by Image J. (***) indicates that the phosphorescence/fluorescence intensity of PLNP-PS is significantly different between 1 h and 4 h ($P < 0.001$)

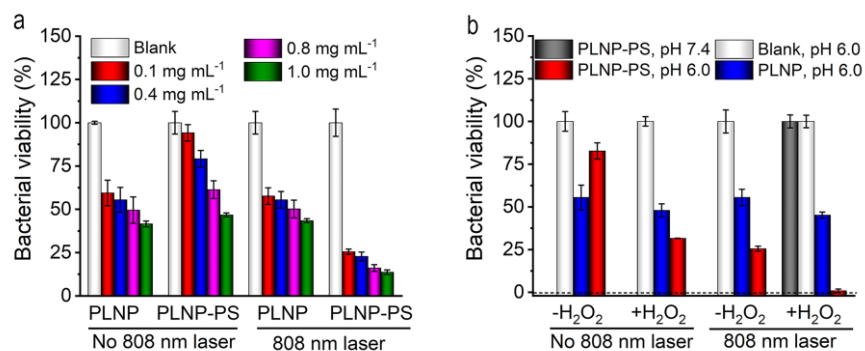


Figure S17. Dark toxicity and CDT/PDT synergistic antibacterial effect to *S.aureus*. (a) Dark toxicity of different concentrations of PLNP and PLNP-PS with or without 808 nm laser (0.6 W cm⁻², 10 min). (b) CDT/PDT synergistic antimicrobial effect of PLNP-PS (0.4 mg mL⁻¹) with or without H₂O₂ (2 μmol L⁻¹) and 808 nm laser at pH 7.4 or 6.0 (0.6 W cm⁻², 10 min).

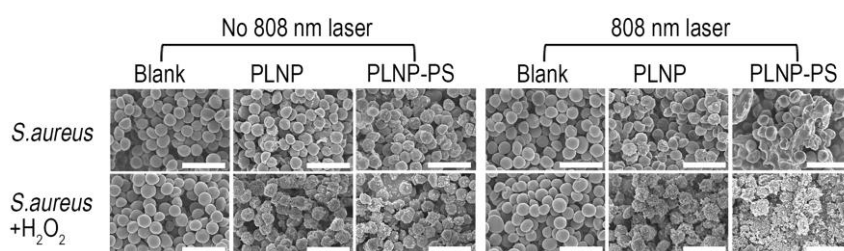


Figure S18. SEM imaging of bacteria incubated with PLNP, PLNP-PS or not in the presence or absence of H₂O₂ (2 μmol L⁻¹) and an irradiation of 808 nm laser (0.6 W cm⁻², 10 min) (Scale bar, 3 μm).

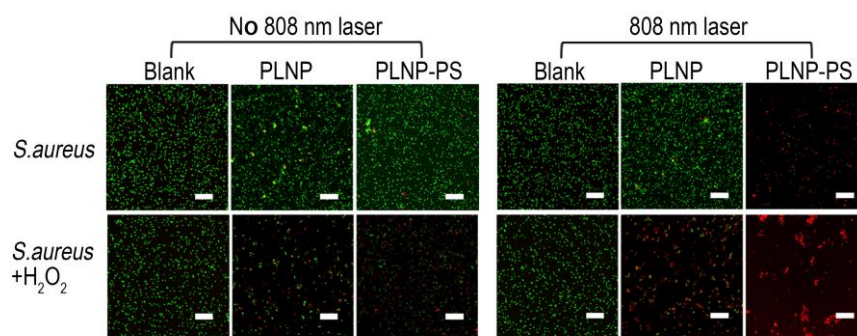


Figure S19. CLSM imaging of bacteria incubated with PLNP, PLNP-PS or not in the presence or absence of H_2O_2 ($2 \mu\text{mol L}^{-1}$) and an irradiation of 808 nm laser (0.6 W cm^{-2} , 10 min). Live and dead bacteria were stained with Calcein-AM or PI in green and red, respectively (Scale bar, 30 μm).

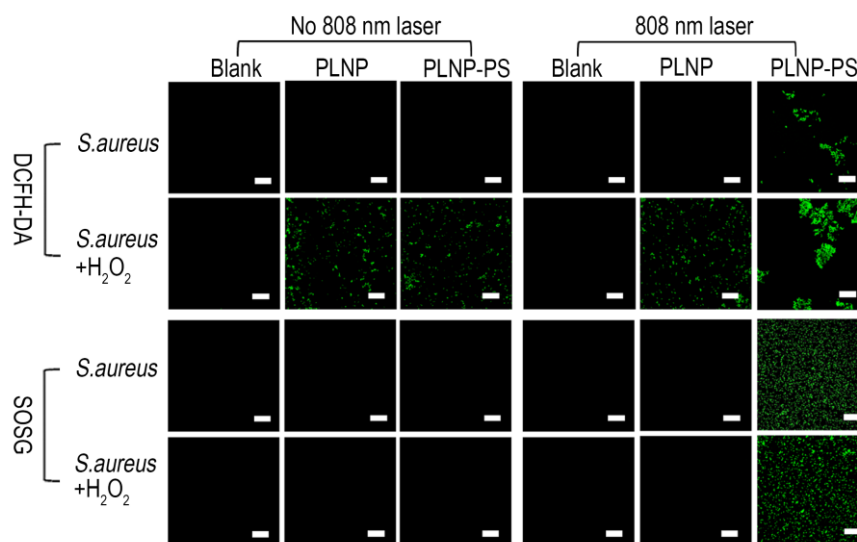


Figure S20. CLSM images of bacterial colonies after different treatments for the detection of ROS or $^1\text{O}_2$, ROS or $^1\text{O}_2$ were detected by DCFH-DA and SOSG, respectively (Scale bar, 30 μm).

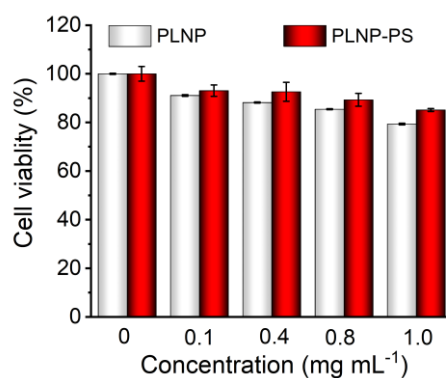


Figure S21. Cell viability of 3T3 cells incubated with PLNP or PLNP-PS.

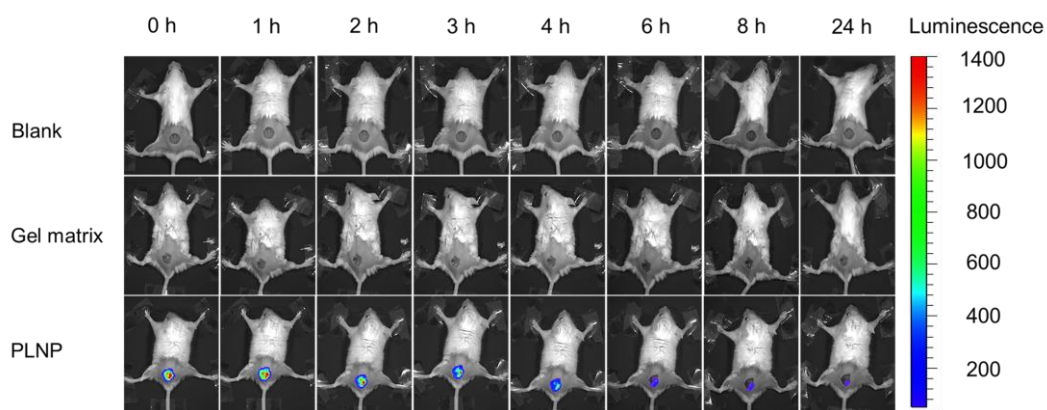


Figure S22. Phosphorescence images of wound in mice coated with nothing, gel matrix, PLNP gel and PLNP-PS gel.

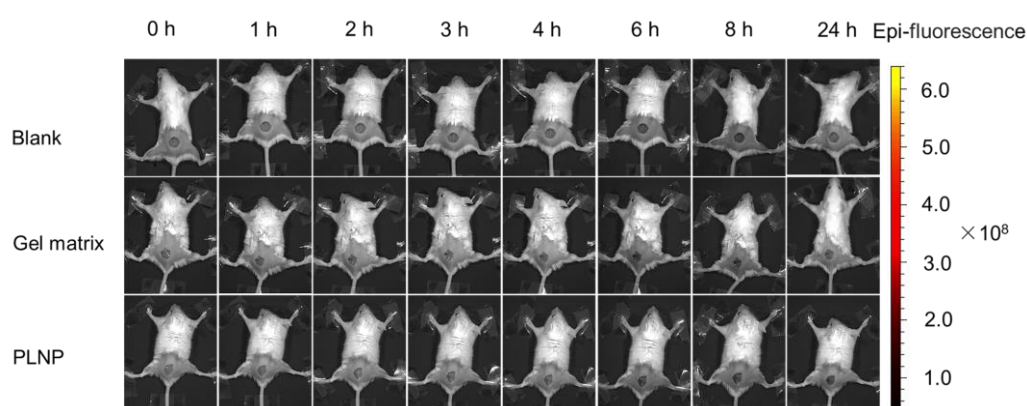


Figure S23. Fluorescence images of wound in mice coated with nothing, gel matrix, PLNP gel and PLNP-PS gel.

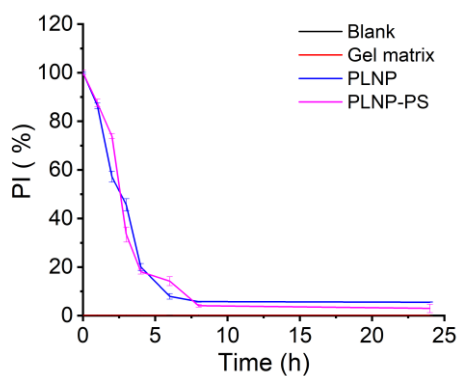


Figure S24. Time-dependent phosphorescence intensity changes of wound in mice coated with PLNP gel and PLNP-PS gel. $PI = P/P_0$, P_0 is the initial phosphorescence intensity of PLNP-PS, while P is the phosphorescence intensity of different groups at a certain time.

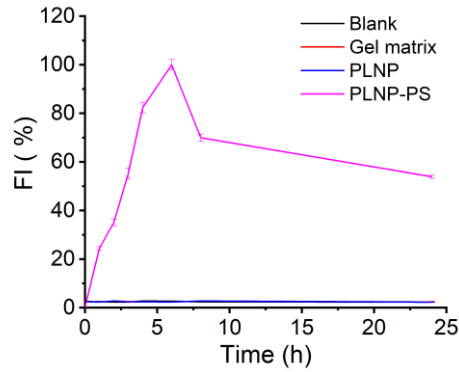


Figure S25. Time-dependent fluorescence intensity changes of wound in mice coated with PLNP gel and PLNP-PS gel. $FI = F/F_0$, F_0 is the strongest fluorescence intensity of PLNP-PS, while F is the fluorescence intensity of different groups at a certain time.

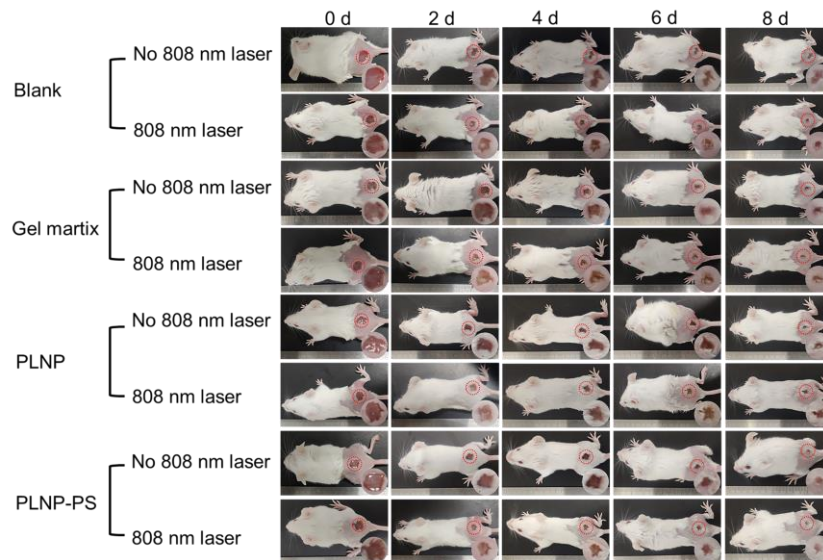


Figure S26. Representative photographs of the mice after treatments for 8 days.

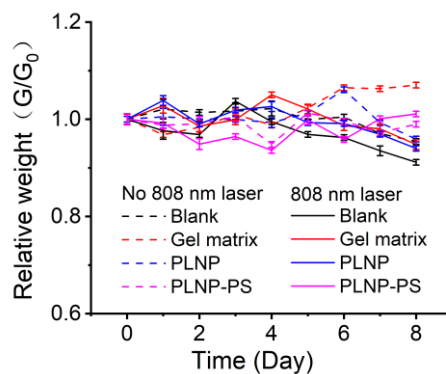


Figure S27. Time-dependent relative body weight of mice under various treatments. G_0 is the initial weight of mice of different groups, while G is the weight at a certain therapy point.

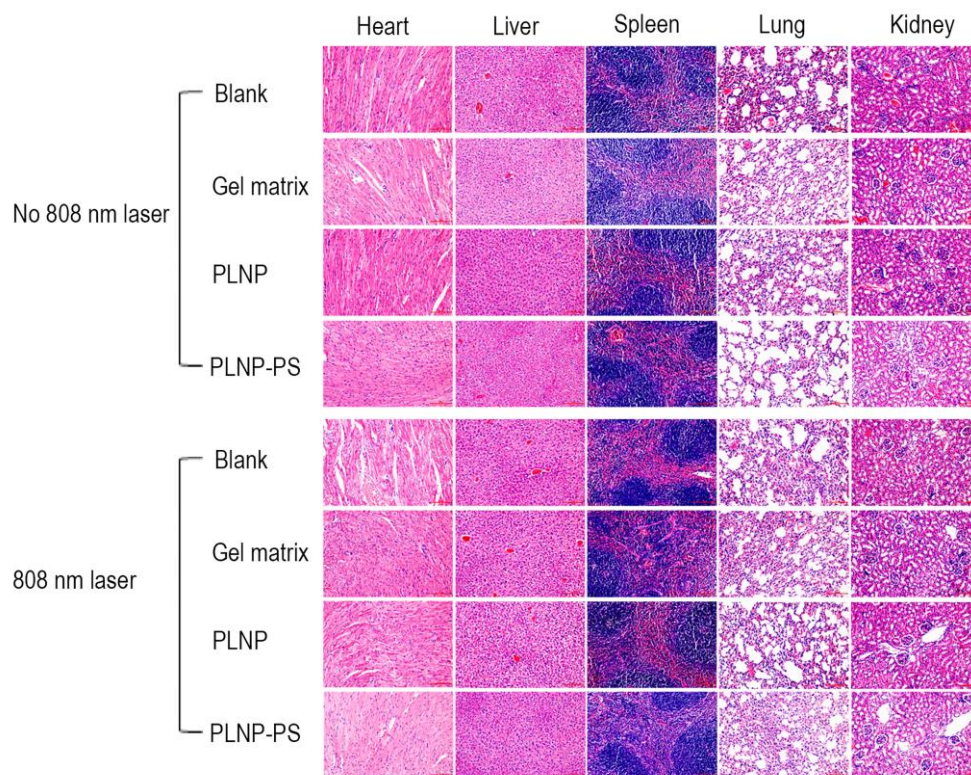


Figure S28. H&E staining of main organs of mice after various treatments for 8 days.